Electrical Conductance of Hydrophobic Membranes or What Happens below the Surface

Ivan Vlassiouk,[†] Fabian Rios,[†] Sean A. Vail,[‡] Devens Gust,[‡] and Sergei Smirnov*[,†]

Department of Chemistry and Biochemistry, New Mexico State University, Las Cruces, New Mexico 88003, and Department of Chemistry and Biochemistry, Arizona State University, Tempe, Arizona 85287

Received January 7, 2007. In Final Form: March 8, 2007

Nanoporous alumina membranes rendered hydrophobic by surface modification via covalent attachment of hydrocarbon or fluorocarbon chains conduct electricity via surface even when the pores are not filled with electrolyte. The resistance is many orders of magnitude higher than for electrolyte-filled membranes and does not depend on the electrolyte concentration or pH, but it does depend on the type of hydrophobic monolayer and its density. The corresponding surface resistance varies from greater than 10^{18} Ω per square to less than 3×10^9 Ω per square. When the hydrophobic monolayer contains a small proportion of photoactive spiropyran that is insufficient to switch the surface to hydrophilic after spiropyran photoisomerization to the merocyanine form, the membrane resistance also becomes light-dependent with a reversible increase of surface resistance by as much as 15%. Surface conduction is ascribed to hydration and ionization of the alumina surface hydroxyls and the ionizable groups of the hydrophobic surface modifiers.

Introduction

Investigation and utilization of hydrophobic surfaces for various applications has gained new momentum recently.[1−9] Hydrophobicity is a fundamental property that controls interactions between nonpolar substances and water. These interactions in turn are responsible for numerous physical and biophysical phenomena. Hydrophobicity has been studied extensively, but many aspects are still not well understood. The strong attraction between water molecules due to hydrogen bonding makes their interaction with nonpolar substances unfavorable. Poor wetting of hydrophobic surfaces by water can be observed experimentally as a large contact angle between a water droplet and a hydrophobic surface. Theoretical calculations predict a thin layer of low-density water near hydrophobic surfaces[10−13] but experiments do not always agree with that.[16] Surface roughness and porosity amplify wetting phenomena—hydrophilic surfaces become superhydrophilic (or ultrahydrophilic), and hydrophobic surfaces become superhydrophobic (or ultrahydrophobic).[17] The contact angle, θ, on superhydrophobic surfaces can be very close to 180°.[18] Surface topography is a generally more important factor than porosity—brushes typically have a greater θ than porous membranes of the same material because of the topological advantage in realization of the contact line between water and the surface. Nevertheless, a membrane with hydrophobic pores will avoid wetting if the pores are of a small size.[1−5,7,8] The latter fact is successfully used in the textile industry.[19] Water intrusion into the pores becomes possible if the pressure gradient at the pore mouth, ΔP, can overcome the surface tension:

$$\Delta P > \frac{4|\Delta\gamma|}{d} \tag{1}$$

where d is the pore diameter and $\Delta\gamma$ is the difference between the wall/vapor surface tension, γ_{wv}, and the wall/liquid surface tension, γ_{wl}. The value of $\Delta\gamma$ is related to the contact angle on the pore walls, θ, via the Young equation:

$$\Delta\gamma \equiv \gamma_{wl} - \gamma_{wv} = \gamma \cos\theta \tag{2}$$

where γ is the liquid/vapor surface tension. If an electrolyte is used instead of water, its intrusion into the pores would electrically short the opposite sides of an otherwise highly resistive dry membrane. This effect can be used for various sensor applications.

In studying the phenomenon of electrical conductance through hydrophobic nanoporous membranes we and others noted that apparently hydrophobic membranes could still exhibit electrical conductance.[1,2,5,19] Martin and co-workers[1,2] have not discussed this issue and concentrated on the effect of the conductance increase when interacted with amphiphiles, but in a recent article by Ku et al.[19] the authors concluded that "the conduction was due primarily to a small number of "hydrophilically defective" pores in membranes modified by long-chain alkylsilanes and both hydrophilic defects and surface conduction in pores modified by short-chain alkylsilanes." The membrane impedances measured by them were orders of magnitude smaller than those reported by Steinle et al.[1] and what we typically measure and report in this article.

* To whom correspondence should be addressed. E-mail: snsm@nmsu.edu.
[†] New Mexico State University.
[‡] Arizona State University.

(1) Steinle, E. D.; Mitchell, D. T.; Wirtz, M.; Lee, S. B.; Young, V. Y.; Martin, C. R. *Anal. Chem.* **2002**, *74*, 2416−2422.
(2) Lee, S. B.; Martin, C. R. *J. Am. Chem. Soc.* **2002**, *124*, 11850−11851.
(3) D'Andrea, S. C.; Fadeev, A. Y. *Langmuir* **2006**, *22*, 3962−3963.
(4) Helmy, R.; Kazakevich, Y.; Ni, C.; Fadeev, A. *J. Am. Chem. Soc.* **2005**, *127*, 12447.
(5) Vlassiouk, I.; Park, C.-D.; Vail, S. A.; Gust, D.; Smirnov, S. *Nano Lett.* **2006**, *6*, 1013−1017.
(6) Genzer, J.; Efimenko, K. *Science* **2000**, *290*, 2130−2133.
(7) Mugele, F.; Baret, J.-C. *J. Phys. Cond. Matter*. **2005**, *17*, R705−R774.
(8) Yoon, J.-Y.; Garrell, R. L. *Anal. Chem.* **2003**, *75*, 5097−5102.
(9) To, N.; Krupenkin, J. A.; Taylor, T.; Schneider, M.; Yang, S. *Langmuir* **2004**, *20*, 3824−3827.
(10) Lum, K.; Chandler, D.; Weeks, J. *J. Phys. Chem.* **1999**, *103*, 4570−4577.
(11) Lum, K.; Chandler, D. *Int. J. Thermophys.* **1998**, *19*, 845−855.
(12) Lum, K.; Luzar, A. *Phys. Rev. E* **1997**, *56*, R6283−R6286.
(13) Luzar, A. *J. Phys. Chem. B* **2004**, *108*, 19859−19866.
(14) Seo, Y.-S.; Satija, S. *Langmuir* **2006**, *22*, 7113−7116.
(15) Schwendel, D.; Hayashi, T.; Dahint, R.; Pertsin, A.; Grunze, M.; Steitz, R.; Schreiber, F. *Langmuir* **2003**, *19*, 2284−2293.
(16) Gao, L.; McCarthy, T. J. *J. Am. Chem. Soc.* **2006**, *128*, 9052−9053.
(17) Feng, X. J.; Jiang, L. *Adv. Mater.* **2006**, *18*, 3063−3078.
(18) Gao, L.; McCarthy. *Langmuir* **2006**, *22*, 5998−6000.
(19) Ku, A. Y.; Ruud, J. A.; Early, T. A.; Corderman, R. R. *Langmuir* **2006**, *22*, 8277−8280.

10.1021/la070038q CCC: $37.00
Published on Web 06/02/2007

Our investigation of this phenomenon presented here studies the conductance through hydrophobic membranes prepared by various methods of surface modification. We point out that the correlation between the hydrophobicity and the electrical resistance is not straightforward and the latter is strongly affected by the hydrolyzable groups underneath the hydrophobic tails of molecular surface modifiers. These groups are also responsible for contact angle hysteresis and render the membrane wetting sensitive to pH.

Our conclusion is opposite to that of Ku et al.:[19] hydrophobic membranes do have intrinsic electrical conductance, not by electrolyte intruding into the imperfect pores but via intrinsic surface conductance of the walls. Appreciation of this phenomenon is crucial for designing ionic conductance sensors based on nanoporous membranes. It also offers new insights into the nature of contact angle hysteresis on hydrophobic surfaces and could assist in the design of polymeric membranes for fuel cells.

Experimental Section

Most of the electrical impedance measurements of the membranes were performed in a glass U-cell with 1 cm^2 of open cross section using a CH 604B electrochemical workstation (from CH Instruments). The membrane formed a barrier between two volumes of the cell containing typically 1.0 M potassium chloride in freshly distilled water at pH 7. Two Ag/AgCl electrodes were in close proximity to the membrane, and a low voltage (<5 mV) was employed for AC impedance measurements at frequencies from 0.1 to 10^5 Hz. A perfectly wetted unmodified membrane in this cell is measured as having 100 Ω of resistance (with 1.0 M KCl), which corresponds to the minimum measurable resistance, R_{min}, for the cell. In experiments including photoexcitation, a plastic cell[5] with 0.3 cm^2 cross section of open membrane area and a tighter placement of Ag/AgCl paste electrodes with $R_{min} = 17$ Ω was used as well. For membrane resistances not exceeding 10 MΩ, a frequency of 100 Hz was used for monitoring impedance variation with time; lower frequencies were chosen for the higher membrane resistances to ensure monitoring of the resistive component.

IR spectra were measured using a Perkin-Elmer Spectrum One FT-IR spectrometer with 0.1 cm^{-1} spectral resolution. Contact angles were measured between a tangent to the surface of a 1 μL water droplet and the substrate using the sessile drop method with a homemade apparatus.

We have previously demonstrated that flat silica and nanoporous alumina membrane surfaces can be modified with alkoxysilanes,[5,20−25] and established that one can achieve dense monolayer coverage. In the case of flat surfaces,[24,25] the density of covalently attached molecules, $\sim 2-4 \times 10^{14}$ cm^{-2}, was very close to that of surface hydroxyl groups, $4-5 \times 10^{14}$ cm^{-2}. Immobilization from dry solvents prevents alkoxysilane polymerization in solutions and ensures less than monolayer coverage. After hydrolyzing unreacted alkoxy groups of the silanes and repeating silanization, a close-to-monolayer coverage can be achieved with the density increasing by ~1.5 times as compared to the first step to reach $3-4 \times 10^{14}$ cm^{-2} and likely promote lateral polymerization between neighboring silanes.[24] Additional hydrolysis and silanization after that produce no measurable effect. A similar two-step silanization approach was used here for hydrophobic surface modification. Disc-shaped alumina filter membranes with 200 nm pores (60 μm thick, from Whatman)

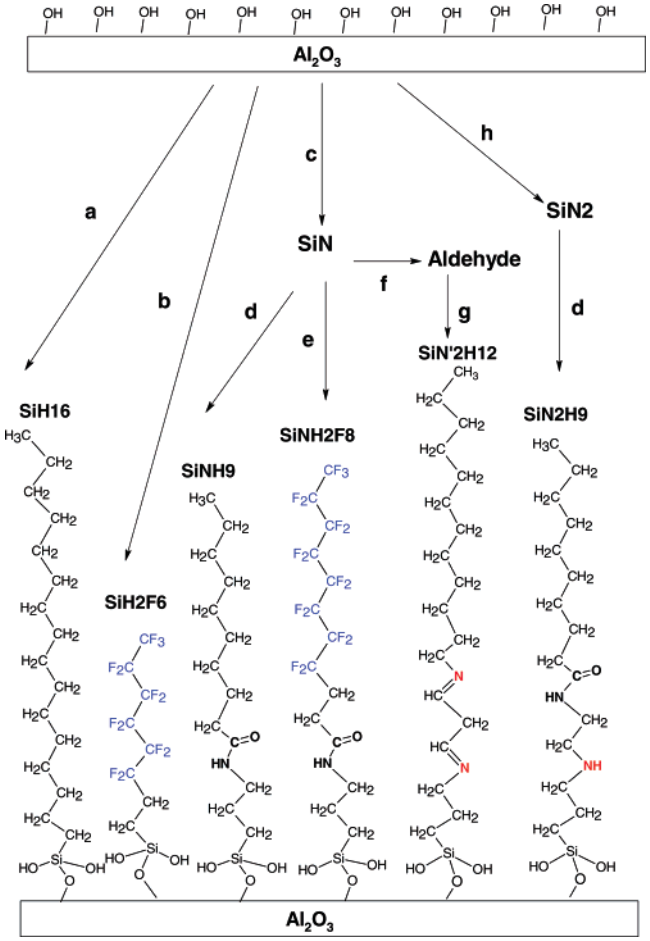

Figure 1. Sketch of the immobilized hydrophobic molecular modifications used in this study with their labels and procedures: (a) hexadecyltrimethoxysilane from toluene; (b) 1*H*,1*H*,2*H*,2*H*-perfluorooctyltrichlorosilane from toluene; (c) 'amination' using aminopropyl trimethoxysilane in toluene; (d) decanoic acid + EDC in ethanol; similar for palmitic acid; (e) fluoroundecanoic acid + EDC in ethanol; (f) 8% aqueous gluteraldehyde; (g) decylamine from water; (h) 'amination' using aminoethyl-aminopropyl trimethoxysilane. A blue color emphasizes highly hydrophobic fluorinated tails, and a red color identifies amines that are potentially charged at normal pH. Nitrogens from amide groups (bold black) are neutral in a broad range of pH. For simplicity, we draw Si connected to the surface via a single Si−O bond because two-bond connections have low probability. The remaining two bonds are presented as hydroxyls, but at high densities many neighboring silanes form lateral Si−O−Si bonds.

were treated using five different modification schemes (see Figure 1) to make their surface hydrophobic. In the first scheme (step *a* in Figure 1), the membrane surface was directly silanized with hexadecyltriethoxysilane or octyltriethoxysilane from toluene solution (overnight), as previously described.[24,25] Such membranes are termed SiH16 and SiH8, respectively. In the second scheme (step *b*), the membrane surface was directly silanized overnight with 1*H*,1*H*,2*H*,2*H*-perfluorooctyltrichlorosilane in toluene solution. These membranes are termed SiH2F6. In both cases, the treatment was concluded by overnight baking at 120 °C and repeating the whole cycle after hydrolysis with an ethanol/water mixture to ensure maximal coverage.[24] Double silanization was also used in the other schemes. In these other schemes, the membrane was first aminated using 3-aminopropyl trimethoxysilane[5,25] (step *c*) and then the carboxylic acid ends of either hexanoic, nonanoic, decanoic, or palmitic acid (step *d*) or 2*H*,2*H*,3*H*,3*H*-perfluoroundecanoic acid (step *e*) were coupled to the surface-bound amino groups using EDC coupling agent (1-ethyl-3-(3-(dimethylamino)propyl)carbo-

(20) Vlassiouk, I.; Takmakov, P.; Smirnov, S. *Langmuir* **2005**, *21*, 4776−4778.
(21) Vlassiouk, I.; Krasnoslobodtsev, A.; Smirnov, S.; Germann, M. *Langmuir* **2004**, *20*, 9913−9915.
(22) Szczepanski, V.; Vlassiouk, I.; Smirnov, S. *J. Membr. Sci.* **2006**, *281*, 587−591.
(23) Takmakov, P.; Vlassiouk, I.; Smirnov, S. *Anal. Bioanal. Chem.* **2006**, *385*, 954−958.
(24) Krasnoslobodtsev, A.; Smirnov, S. *Langmuir* **2002**, *18*, 3181−3184.
(25) Krasnoslobodtsev, A.; Smirnov, S. *Langmuir* **2001**, *17*, 7593−7599.

Table 1. Electrical, IR, and Wetting Properties of Alumina Membranes with Different Modifications[a]

modification	θ^a	θ^a after 2 min at low pH	θ^a after 2 min at pH 14	ν_a (CH_2) cm^{-1}	ν_s (CH_2) cm^{-1}	$R_{initial}$ Ω	R_{final} Ω
SiH8	140°	140° (pH 0)	140°	2923.9	2854.4	$>10^{10}$	$6 \pm 2 \times 10^6$
SiH16	140°	140° (pH 0)	140°	2919.4	2850.8	$>10^{10}$	$10 \pm 4 \times 10^6$
SiH2F6	150°	150° (pH 0)	150°			1×10^6	–
SiNH5	115°	40° (pH 0)	95°	2932.6		<100	
SiNH8	130°	80° (pH 0)	130°	2926.9	2857.8	3×10^3	<100
SiNH9	140°	140° (pH 0.5)	140°	2925.3	2855.9	2×10^6	$7 \pm 3 \times 10^5$
SiNH15	140°	140° (pH 0.5)	140°	2924	2854	3×10^7	$8 \pm 4 \times 10^6$
SiN2H9	140°	40° (pH 0.5)	120°	2926.9	2857.4	<100	<100
SiN2H15	140°	50° (pH 0)		2926.0	2857.0	4×10^5	$8 \pm 4 \times 10^4$
SiNH2F8	150°	150° (pH 0)	150°			1×10^8	$3 \pm 1 \times 10^6$
SiN2H2F8	150°	135° (pH 0)	150°			4×10^6	
SiN′2H12	135°			2927.1	2857.2	4×10^3	
SiN	<10°					<100	<100
untreated	<10°					<100	<100

[a] See text for details. Each modification was analyzed on at least three and as many as 15 membranes. [b] Values from Sessile drop method with 1 μL droplet with accuracy ±3°.

diimide).[5,27−32] These membranes are termed SiNH5, SiNH8, SiNH9, SiNH15, and SiNH2F8, respectively. Membranes for which (*N*-2-aminoethyl)-3-aminopropyltrimethoxysilane was used for amination (step h) instead of 3-aminopropyltrimethoxysilane will be termed SiN2H9, SiN2H15, and SiN2H2F8, respectively. The fifth scheme involved activating the aminated surface with an 8% aqueous solution of gluteraldehyde (step *g*)[20,21] followed by coupling with dodecyl amine from aqueous solution (step *g*) to result in an SiN′2H12 membrane. Mixed SiNH9/SiN membranes were prepared via step *d* in Figure 1 by stopping the amide-forming reaction before completion. The amount of material bound to the membrane surface was monitored by IR absorbance in the regions of methylene and hydroxyl absorptions. The mixed SiNH9/SiNspiropyran membranes were prepared using a mixture of decanoic acid and the spiropyran carboxylic acid, 1′-(3-carboxypropyl)-3′,3′-dimethyl-6-nitrospiro-[2*H*-1]benzopyran-2,2′-indoline, in step *d* of Figure 1 to form a complete monolayer.[5] The amount of bound spiropyran was monitored by its UV absorbance.

Overall, more than 70 membranes were analyzed—from as low as 3 to as high as 10 for different modifications

Results

Contact Angle. All modified membranes except SiN demonstrate hydrophobic or ultrahydrophobic (superhydrophobic) behavior—a free-standing small water droplet has a contact angle greater than 120° (the accuracy of our measurements is ±3°) for the most of them (see Table 1). These angles are greater than those for flat surfaces because inhomogeneous topography of membranes (walls and voids) amplifies the contact angle.[9,16−18] Generally, fluorinated modifiers render membranes most hydrophobic, with a contact angle, θ, around 150° for all three that were used. Superhydrophobicity of fluorinated membranes is also revealed in spontaneous movement of droplets on their slightly tilted surfaces; a water droplet bounces off their surfaces with ease. Aliphatic modifiers show broader variation in θ, with maximum $\theta = 140°$ for the longest chains, as shown in Table 1 and Figure 2. This value represents the apparent contact angle

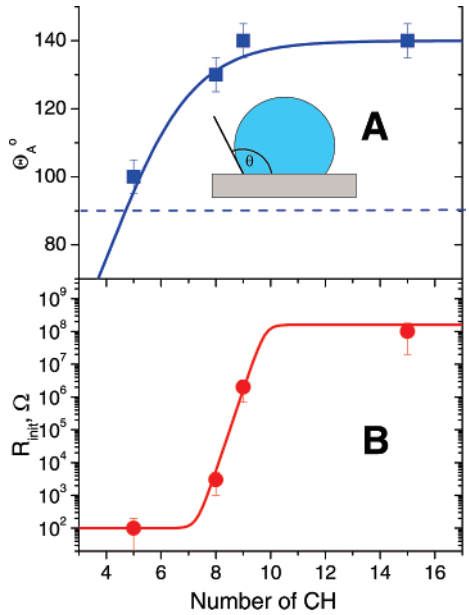

Figure 2. Variation of the contact angle, θ_A (A), and the initial impedance, R_{init} (B), of modified alumina membranes as a function of aliphatic chain length in SiNHn monolayers. The intrinsic cell impedance, ca. 100 Ω, forbids measuring of R_{init} below that value. The lines are only to guide the eyes. The inset illustrates how the contact angle is measured.

from the sessile drop method, which depends on the surface density of immobilized hydrophobic molecules, their nature, and other factors such as pH and exposure time. Over time, the droplet (originally 1 μL in volume) evaporates and the contact line moves in accordance with the hysteresis value of θ. The apparent contact angle starts with close to what is measured in the pendant drop method as the advancing angle, θ_A. The contact line starts moving only after the apparent angle decreases to the value close to that of the receding angle, θ_R. During the first 2 min the evaporation is insignificant, but it becomes noticeable after 4 min.

Bare alumina membranes are unstable in highly acidic and highly basic solutions, but hydrophobically modified membranes can survive in a much broader range of pH. For most of them, the hydrophobic properties are preserved within the range $1.5 < pH < 13.5$. The effect of a strong base (NaOH) is weaker than that of an acid (HCl). At pH 0.5 the contact angle of a SiN2H9 membrane drops to 40° after 2 min from the original value of $\theta = 140°$, while SiNH9 membranes maintain θ well during this time and require pH 0 to drop θ to 45° within 2 min. An SiNH15

(26) Takmakov, P.; Vlassiouk, I.; Smirnov, S. *Analyst* **2006**, *131*, 1248−1253.
(27) Vlassiouk, I.; Takmakov, P.; Rios, F.; Smirnov, S. *J. Phys. Chem. C* **2007**, in press.
(28) Song, X.; Zhai, J.; Wang, Y.; Jiang, L. *J. Colloid Interface Sci.* **2006**, *298*, 267−273.
(29) Rosario, R.; Gust, D.; Garcia, A.; Hayes, M.; Taraci, J.; Clement, T.; Dailey, J.; Picraux, S. *J. Phys. Chem. B* **2004**, *108*, 12640−12642.
(30) Sheng, Y.; Leszczynski, J.; Garcia, A.; Rosario, R.; Gust, D.; Springer, J. *J. Phys. Chem. B* **2004**, *108*, 16233−16243.
(31) Rosario, R.; Gust, D.; Hayes, M.; Jahnke, F.; Springer, J.; Garcia, A. *Langmuir* **2002**, *18*, 8062−8069.
(32) Rosario, R.; Gust, D.; Hayes, M.; Springer, J.; Garcia, A. *Langmuir* **2003**, *19*, 8801−8806.

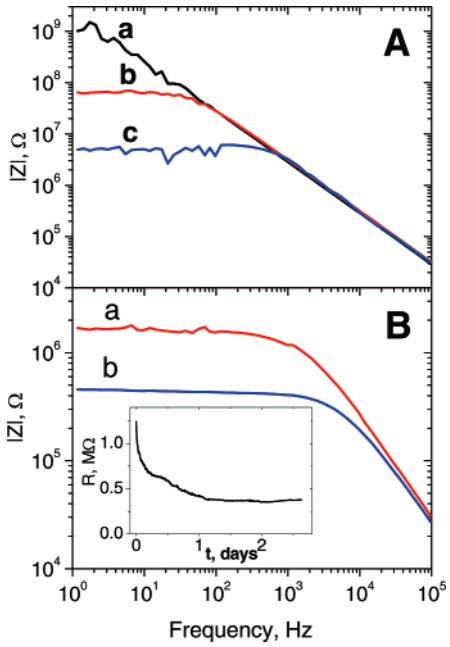

Figure 3. Bode plots for hydrophobic membranes as a function of their aging. (A) SiH16 membrane: (c) upon stabilization after an extended wait; (a, b) two examples right after a membrane in the cell assembly was washed with acetone. (B) SiNH9 membrane: (b) upon stabilization after an extended wait; (a) after washing with acetone. The inset shows an example of SiNH9 membrane resistance evolution (at 100 Hz) after washing with acetone. NB. All measurements were done in 1.0 M KCl; however, the low-frequency resistance does not depend on salt concentration for any of the hydrophobic membranes.

membrane is more resistant, with $\theta = 120°$ after 2 min at pH 0. Fluorinated membranes are exceptional in surviving these harsh conditions. For an SiN2H2F8 membrane, θ dropped insignificantly (to $\theta = 135°$) after 2 min at pH 0, and an SiNH2F8 membrane showed no sign of deterioration, with θ unchanged at 150°. Interestingly enough, almost all membranes, fluorinated or not, survive highly basic conditions (pH 14) with no visible signs of water intrusion until droplet evaporation.

Impedance. The conductive properties of the membranes differ dramatically. As demonstrated by the Bode plots in Figure 3, the frequency dependence of the membrane impedance has a well-defined capacitive component, which is almost identical for all membranes, and a resistive component that varies dramatically: from less than 100 Ω to greater than 10 GΩ. For example, membranes with SiN2H9 modifications show very low electrical resistance (below 100 Ω), despite their quite hydrophobic appearance. If left in electrolyte for a few hours, they eventually wet. The process of water penetration can be expedited by lowering pH, but not as effectively by raising pH. Many membranes show enormously high resistance, greater than 1 MΩ, as would be expected for completely dry membranes. These membranes also remain ultrahydrophobic for a very long time if left in electrolyte. Nevertheless, the initial resistances among membranes differ and for nonfluorinated ones demonstrate the following order: SiH16 ≈ SiH8 > SiNH15 > SiNH9 > SiNH8 > SiN2H15 > SiN′2H12 > SiN2H9, SiNH5, as illustrated by Table 1 and Figures 2−4. A similar trend is observed among fluorinated membranes.

The initial resistance of a membrane typically declines with time and often by as much as an order of magnitude but in all cases when stabilized at a value greater than that of the cell, R_{min}, *the resistance is independent of electrolyte concentration and pH*, at least within the range 3 < pH < 11. However, resistance

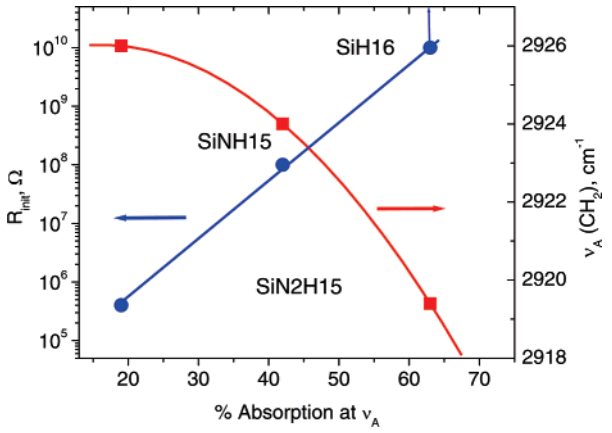

Figure 4. Correlation between the membrane resistance (solid squares), the value of ν_A (solid circles), and the amount of IR absorption at the frequency of asymmetric stretching, $\nu_A(CH_2)$ for three surface modifiers of a similar length. The resistance for SiH16 is the lower limit and the lines are to guide the eyes.

does depend on membrane pretreament and aging. The highest resistances, greater than 10 GΩ, were observed for SiH16 and SiH8. Thoroughly washed with ethanol and dried in the oven right before the impedance measurements, these membranes do not show a resistive component even for frequencies lower than 0.1 Hz. If left in water or electrolyte, their Bode plots remain unchanged for at least 2 days, but then the resistance gradually drops down to ca. 10 MΩ over a period of a week. If left in ambient air, the resistance drops noticeably faster, in 1 day, probably due to impurities in the air. Membranes with other modifications show smaller decline.

Surface modifiers containing heteroatoms, such as SiNH9, SiNH15, SiN2H9, SiN2H15, and SiN2H9, show lower resistances than silanes bearing only polymethylene chains, even when their total length is greater. This could be in part due to a lower surface density of these molecules, but the different characters of the linking groups (amides and amines) probably also enhance surface conductance. Secondary amines are fairly basic and in water carry positive charge at neutral pH, while amides remain neutral. Correspondingly, membranes modified with molecules possessing secondary amines, such as SiN2H9 and SiN2H15, are more conductive than those with only amide linkers. Schiff bases of SiN2′H12 also make the resistance of corresponding membranes quite low. As we have recently reported,[22] secondary amines remaining in a linker contribute to their decreased linker stability on alumina. The increase of the local pH due to the amines promotes accelerated cleavage of Si−O−Al (as well as peptide) bonds to detach molecules from the surface. The surfaces in that case were not hydrophobic, allowing easy water access to the amines.

When different hydrophobic modifiers are compared for the same amine linker, it is apparent that the longer aliphatic and/or fluorinated tails show not only superior hydrophobic behavior but a greater electrical resistance: the resistances decline in the order SiNH2F6 > SiNH15 > SiNH9 > SiNH8 > SiNH5 (see Table 1 and Figure 2). This trend persists even within the series of linkers with secondary amines, SiN2H2F6 > SiN2H15 > SiN2H9.

In general, the initial resistance, $R_{initial}$, of membranes while inside the cell gradually decreases with time (in no more than a day) to a slightly lower value, R_{final}, that is still independent of salt concentration. The exceptions are cases when electrolyte intrudes into membrane (i.e., with resistances lower than R_{min}). The inset in Figure 3B demonstrates this for an SiNH9 membrane.

When available, both initial and final resistances are given in Table 1. This gradual resistance decline correlates with the growth and eventual stabilization of IR absorption in the OH stretching region (a broad band between 2700 and 3600 cm^{-1}) observed for these membranes. At first, when a membrane is dried in the oven, there is a depletion of OH absorption, but eventually, over a period sometimes as long as several days (for purely aliphatic linkers), the absorption partially recovers due to trapping of water vapor, presumably in the vicinity of alumina surface.

On the basis of these facts, we postulate that the electrical conductance through pores of a 'dry' membrane proceeds via the surface of the pore walls. Its independence of salt concentration and correlation with the rise of intensity of hydroxyl IR absorption suggests that water and the products of its dissociation (protons and hydroxide ions) are the likely charge carriers. Higher membrane conductance correlates with increasing sensitivity to acids, which suggests that basic groups on the linkers and the surface (also basic) contribute to charge and water transport.

The phenomenon of electrical conductance in thin water layers at surfaces has been noted before. It was reported that surfaces of oxides and mica are poor electrical conductors with resistances dramatically dependent on humidity.[34,35] At the same time, hydrophobic modification of such surfaces was found to cause a dramatic drop in conductance to the point that it became virtually unmeasurable.[34,35] Because of the small thickness and very high surface area of our membranes, their resistance is scaled down by as much as 7 orders of magnitude compared to sheet resistance, offering a greater sensitivity for very low conductance measurements on such 'nonconductive' hydrophobic surfaces. The conductance of an electrolyte is many orders of magnitude higher than that of the pore walls—even a deionized water-filled membrane would have resistance of only 0.1 MΩ. Thus, one can use the pore resistance for monitoring the extent to which the pores are filled with electrolyte[5,27] appreciating that this conductance is very sensitive to the type of chemistry used for rendering the surface hydrophobic.

Recently, we investigated water intrusion into membranes with a hydrophobic photosensitive surface by monitoring electrical conductance.[5] The photosensitive surface was prepared as a mixed SiNH9/SiNspiropyran monolayer, where the relative amount of spiropyran was varied over a broad range. Upon irradiation with 337 nm light, the spiropyran undergoes photoisomerization into its zwitterionic merocyanine form (Figure 5) but can be converted back into the spiro form by irradiation at 532 nm. The merocyanine form is more polar and causes a reduction of the surface tension of water. If the relative concentration of spiropyran is sufficient, its photoexcitation can decrease the contact angle below 90°, thus allowing water intrusion into the pores. We now report that at low spiropyran concentrations, when its conversion into the merocyanine form is insufficient to turn the surface hydrophilic, the membrane conductance is also photoswitchable but to a much smaller degree. Figure 5 shows that for a relative spiropyran concentration of less than 5% of its maximum (absorbance at the isosbestic point is <0.03 as compared with the maximum value of 0.8) the membrane resistance *increases* after converting the spiropyran into its polar, merocyanine form. Moreover, the effect is reversible—the resistance drops back after the recovery of the original spiro form. The effect is much smaller (~15% for the data in Figure 5) and *opposite* to that observed with water

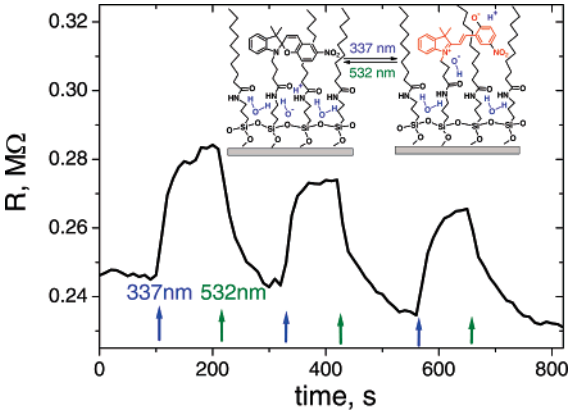

Figure 5. Variation of the resistance (|*Z*| at 100 Hz) of alumina membranes modified with a mixed SiNH9/SiNspiropyran monolayer as a function of laser irradiation of different wavelengths. The relative concentration of spiropyran is very low, ~4% of its maximal, which retains the membrane hydrophobic. Upon irradiating with 337 nm (blue arrow) spiropyran converts into the zwitterionic merocyanine form, but after 532 nm irradiation returns to the spiro form. More polar merocyanine better captures the free ions and thus increases the membrane resistance. The inset shows the forms of spiropyran.

intrusion, which at the maximum was almost 100-fold.[5] What is the cause for such conflicting behavior? The surface conductance phenomenon is consistent with conjecture that spiropyran in its merocyanine form is better able to efficiently bind charge carriers inside the surface monolayer than is the neutral spiro form. This strong interaction apparently disrupts the continuity of conductive chain of charge carriers.

Different linking groups vary in their surface coverage density, which can leave some hydroxyls of the alumina surface exposed. For modifications involving step *c* in Figure 1, this can mean that not all amines necessarily react with carboxylic acid. To further delineate the effect of amino groups on conductance and its correlation with surface hydrophobicity we analyzed membranes with mixed SiNH9/SiN monolayers prepared by reacting aminated membranes with decanoic acid (step *d* in Figure 1) for different times. The concentration of hydrophobic tails was measured by IR absorption of $\nu_a(CH_2)$ at ~2920 cm^{-1} and normalized to its maximum value reached after ~15 h of reaction. As the degree of hydrophobic coverage increases, the contact angle continuously increases and eventually reaches $\theta = 140°$ for SiNH9.

As Figure 6 illustrates, there is a broad range of densities of aliphatic groups above 70% of the maximum, where the hydrophobic appearance of the membrane is accompanied by measurable conductance. For relative surface densities between 82% and 100% (or surface density of amines up to 18%) the membrane resistance varies over 4 orders of magnitude. The resistance in that range still does not depend on electrolyte concentration, which means that its decline with increasing density of amines is not due to the rising probability of some pores being filled with electrolyte. Instead, it reflects the increasing conductance of the pore walls. The latter drastically increases with the surface density of amines, N_{amines}. If fitted as a simple exponential:

$$R = R_{max} \exp(-N_{amines}/N_0) \quad (3)$$

the resistance demonstrates a very sharp decline with a small increment—the characteristic density of decline, of only $N_0 \approx$ 2%. Equation 3 emphasizes that the capacitive component of

(33) Bunker, B.; Kim, B.; Houston, J.; Rosario, R.; Garcia, A.; Hayes, M.; Gust, D.; Picraux, S. *Nano Lett.* **2003**, *3*, 1723−1727.
(34) Guckenberger, R.; Heim, M.; Cevc, G.; Knapp, H. F.; Wiegrabe, W.; Hillebrand, A. *Science* **1994**, *266*, 1538−1540.
(35) Heim, M.; Cevc, G.; Guckenberger, R.; Knapp, H. F.; Wiegrabe, W. *Biophys. J.* **1995**, *69*, 489−497.

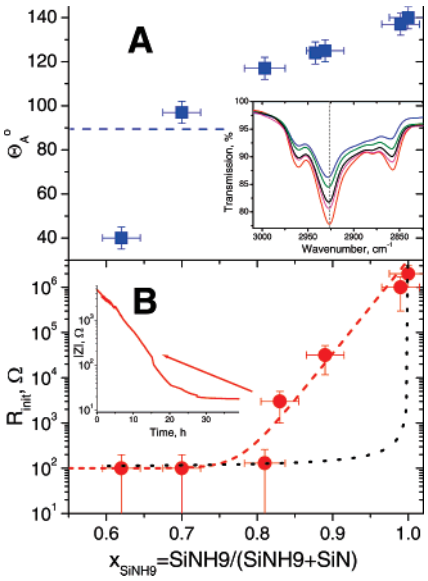

Figure 6. Variation of the contact angle, θ_A (A), and the initial resistance, R_{init} (B), of modified membranes as a function of the SiNH9 hydrophobic fraction in mixed SiNH9/SiN modifiers. Intrinsic cell resistance, ca. 100 Ω, forbids measuring of R_{init} below that value. The insert in (A) shows CH stretching region of IR absorption used to monitor the density; the vertical dashed line accentuates the ν_a peak gradual shift to lower frequencies with improved coverage. The insert in (B) shows the kinetics of the resistance decline for the membrane with $R_{init} = 4 \times 10^3 \Omega$. Resistance of the membranes with $x_{SiNH9} > 0.82$ is independent of electrolyte concentration. The dashed line is the best fit using eq 3 with $R_{max} = 4$ MΩ and $N_0 = 2.1\%$. Dotted line represents solution to eq 6.

membrane impedance is not affected and all the changes are observed only for resistance (the low-frequency plateau in the Bode plot).

IR Absorption. Additional information about surface hydration was obtained from IR spectra of the membranes. Membranes themselves impose some artifacts in the spectra: the interference pattern due to membrane thickness appears in the IR spectra as oscillations of up to 5% of transmittance and varies among membranes; other irregularities include lack of membrane transmittance below 1200 cm^{-1} and erroneous hydroxyl absorption between $\nu(OH) \approx 2700-3700$ cm^{-1}. The latter appears as enhanced transmittance when compared to an untreated membrane and partially recovers over a period of tens of hours due to trapping of water vapor, as described above.

All these hinder the accuracy of determining the intensities and frequencies of resonance lines. Nevertheless, CH_2 stretching[36−39] (asymmetric around $\nu_a(CH_2) \approx 2930$ cm^{-1} and symmetric near $\nu_s(CH_2) \approx 2860$ cm^{-1}), and CH_3 stretching around 2960 cm^{-1} are well recognizable, especially for longer aliphatic chains. The frequencies can be determined with sufficient accuracy, but absolute integral intensities are difficult to evaluate except for the intensities for the same linker under different conditions. It has been previously shown[36] that for a series of *n*-alkyl thiols on gold, the peak intensities of CH_2 stretching do not well represent the variation of monolayer densities in that series. The peaks positions were found to be indicative of the intermolecular environment of the alkyl chains in the assemblies: blue-shifting of both $\nu_a(CH_2)$ and $\nu_s(CH_2)$ correlated with more crystalline-like assembly and was observed for long chains. A crystalline polymethylene chain has a $\nu_a(CH_2)$ frequency (2920 cm^{-1}) that is 8 cm^{-1} lower than that for the liquid state.[36,37] Similarly, $\nu_s(CH_2)$ shifts by almost 6 cm^{-1}, from 2850 to 2856 cm^{-1}, upon polymer melting. Regularly organized flat surfaces promote the all-trans conformation and a crystal-like arrangement of the hydrocarbon tails. Because of the metallic gold surface, molecular orientation significantly affects the intensities of different vibrational modes[36,39] and probably contributes to greater peak shifts than those observed for bulk samples.

Alumina membranes have fairly rough and curved surfaces inside nanopores; the distribution of surface hydroxyls, at which attachment of surface modifiers takes place, is also far from regular. Thus one would expect less order in a self-assembled monolayer relative to gold, at least in terms of its pseudo-crystalline appearance. Our data show that this is generally correct but, as the case with the SiH16 modifier demonstrates, high-quality monolayers can be achieved that have stretching frequencies $\nu_a(CH_2) = 2919$ cm^{-1} and $\nu_s(CH_2) = 2851$ cm^{-1} very close to those of similar length thiols on gold[36] and silanes on oxidized silicon wafers.[40] The shorter silane modifier SiH8 appears more disordered, as illustrated by its higher frequency $\nu_a(CH_2) = 2924$ cm^{-1}. A similar correlation of increasing disorder with shortening of the aliphatic chain length was observed for alkyl thiols on gold.[36,39]

Complex linkers generally have higher $\nu_a(CH_2)$ values, but the trend was recognizable for them as well. In a series of SiNHn modifiers $\nu_a(CH_2)$ drops gradually from 2933 cm^{-1} in SiNH5 to 2927 cm^{-1} in SiNH8, to 2925 cm^{-1} in SiNH9, and to 2924 cm^{-1} in SiNH15. One can recognize this trend even in the difference between SiN2H9 and SiN2H15 with their respective $\nu_a(CH_2) = 2927$ and 2926 cm^{-1}.

In accordance with the previously established trend,[36] a decreasing frequency of $\nu_a(CH_2)$ reflects improved all-trans alignment of methylene chains with their increasing length. Obviously, the quality of this alignment also depends on the density of molecular coverage. The inset in Figure 6A demonstrates that $\nu_a(CH_2)$ shifts to lower values with increasing density of coverage in SiNH9, which correlates with the increasing water droplet contact angle and the membrane resistance.

Even though evaluation of total coverage by comparing IR absorbance for different modifiers is ambiguous due to the above-mentioned limitations, linkers with similarly long aliphatic tails can probably be analyzed with less ambiguity. A careful look reveals that full coverage with a SiN2H15 monolayer is never as high as with SiNH15 and that both are lower than with an SiH16 modifier (see Figure 4). It holds true for SiN2H9 and SiNH9 and does not improve by repeating silanization steps. The reason for that is not totally clear especially since we did not observe such a significant difference on flat silica surfaces.[24,25] The effect is likely a combination of enhanced hydrogen bonding of amines to the surface and poorer packing alignment in SiN2Hn that both prevent the coating from reaching a mature dense monolayer. As Figure 4 suggests, both resistance, *R*, and $\nu_a(CH_2)$ can be correlated with the amplitude of absorption at $\nu_a(CH_2)$, even though the contact angles for these membranes are almost the same.

(36) Porter, M. D.; Bright, T. B.; Allara, D. L.; Chidsey, C. E. D. *J. Am. Chem. Soc.* **1987**, *109*, 3559−3568.
(37) Snyder, R. G.; Strauss, H. L.; Elliger, C. A. *J. Phys. Chem.* **1982**; *86*, 5145−5150.
(38) Snyder, R. G.; Maroncelli, M.; Strauss, H. L.; Hallmark, V. M. *J. Phys. Chem.* **1986**, *90*, 5623−5630.
(39) Laibinis, P. E.; Whitesides, G. M.; Allara, D. L.; Tao, Y.-T.; Parikh, A. N.; Nuzzo, R. G. *J. Am. Chem. Soc.* **1991**, *113*, 7152−7167.
(40) Le Grange, J. D.; Markham, J. L.; Kurkjian, C. R. *Langmuir* **1993**, *9*, 1749−1763.

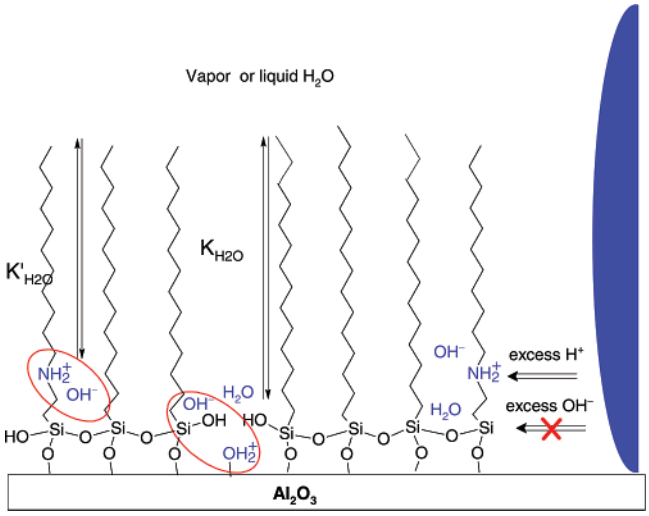

Figure 7. Illustration of multifaceted wetting equilibria near a hydrophobically modified wall. Equilibrium for water adsorption depends on the concentration of hydrophilic groups near the surface and their type. Reaching this equilibrium can take days. The dissociation of ionizable hydrophilic groups (amines on linkers or surface hydroxyls) and water is incomplete—the circles represent strong Coulombic attraction between the resulting ions in the ion pairs. Highly acidic solutions promote surface wetting, but bases have insignificant effect, in agreement with pH dependence for ionization of amines and hydroxyls of alumina.

Discussion

It is clear from our data that the hydrophobic appearance of a membrane surface, as measured by large contact angles, θ, and the corresponding lack of electrolyte intrusion into the membrane has limited correlation with its electrical conductance. We emphasize that lack of the membrane resistance dependence on the concentration of electrolyte and pH not only eliminates the 'poor pores' mechanism of Ku et al.[19] but demonstrates that charge carriers responsible for surface conductance are intrinsic to the surface. Unwetted, "dry" membranes still conduct electricity and, as membranes with small amount of spiropyran in the surface monolayer demonstrate, that conductance depends on the concentration of free carriers intrinsic to the monolayer and can be reversibly altered by the switching polarity of spiropyran. The charge carriers are not the ions of electrolyte and should originate from dissociation of water traces and ionizable groups of modifiers.

Thus, water and charge carriers must be present below the membrane surface, and these are responsible for conductivity. This is not too surprising. After all, if water did not penetrate deeper than the outermost methyl of the aliphatic chain, there should be no dependence of the contact angle on the aliphatic chain length. Although the experimentally observed θ for alkanethiol monolayers on gold does indeed saturate beyond nine carbon atoms in the aliphatic chain, it has a weak dependence on the number of methylene groups for shorter chains. This is believed to be caused by imperfect packing for chains of those lengths.[36]

Our results show that the packing density of a monolayer affects the membrane conductance much more strongly than the contact angle (see Figures 4 and 6). The voids in the hydrophobic coverage are too minute in size for a significant drop in surface energy interaction with water, but they can and do expose hydrophilic groups to water vapor. These groups are hydroxyls on the alumina surface and amines (primary or secondary) on the linkers themselves or as residual groups from incomplete reactions (see also Figure 7). They not only 'attract' water but also are ionizable, i.e., capable of promoting water dissociation and thus electrical conductance:

$$R{-}NH_2 + H_2O \rightarrow R{-}NH_3^+ + OH^- \quad (4)$$

$$R{-}NH_2 + H_3O^+ \rightarrow R{-}NH_3^+ + H_2O \quad (5)$$

$$R{-}NH_2 + OH^- \not\rightarrow R{-}NH^- + H_2O \quad (6)$$

$$Surf{-}OH + H_2O \rightarrow Surf{-}OH_2^+ + OH^- \quad (7)$$

$$Surf{-}OH + H_3O^+ \rightarrow Surf{-}OH_2^+ + H_2O \quad (8)$$

$$Surf{-}OH + OH^- \not\rightarrow Surf{-}O^- + H_2O \quad (9)$$

Reactions 4, 5, 7, and 8 have significant equilibrium constants, while reactions 6 and 9 do not proceed at normal pH. For the same reason, intrusion of electrolyte into the pores is more susceptible to low pH when reactions 5 and 8 are significantly shifted to the right and thus more water can be stabilized near the ionizable groups. Other hydrophilic groups in the modifiers such as amides do not contribute as strongly to the membrane conductance because of their ambivalence at neutral pH.

Since membrane conductance proceeds via the pore walls and is independent of electrolyte, one may wonder if it is possible to measure it between electrodes on a flat modified surface. The latter is usually called the sheet resistance, R_s. Numerous pores connected in parallel make membrane resistance, R, many orders of magnitude smaller than the sheet resistance, R_s:

$$R = R_s \frac{1}{N}\frac{L}{\pi d} = R_s \frac{\pi d^2/4}{\alpha S}\frac{L}{\pi d} = R_s \frac{dL}{4\alpha S} \approx 3 \times 10^{-8} R_s \quad (10)$$

Here calculations were made for a membrane thickness, L, of 60 μm, and a diameter of its pores, d, of 200 nm. The number of parallel connected pores, N, in the exposed cross-section area, $S = 1$ cm^2, is calculated from a single pore cross-section area, $\pi d^2/4$, and the portion of the cross-section covered by pores, $\alpha \approx 0.9$. Thus, the calculated lower limit for sheet resistance of an SiH16 modified surface exceeds R_s(SiH16) > 10^{18} Ω per square and the experimental lower limit, $R_{min} \approx 100$ Ω, corresponds to $R_s \approx 3 \times 10^9$ Ω per square. Measuring such high resistances is next to impossible on flat surfaces.

In the next part we will discuss the mechanisms of surface conductance with the goal of trying to estimate the sheet resistance of hydrophobically modified surfaces. Ascribing the sheet resistance to ionic substances presented on a surface at (surface) concentration N_s should result in the sheet resistance being inversely proportional to N_s and the ion mobility, μ. For the latter it is common to use the Einstein relation expressing μ via a diffusion coefficient, D_s: $\mu = eD_s/k_BT$. Thus, the sheet resistance is inversely proportional to both N_s and D_s:

$$R_s(\Omega) = \frac{k_B T}{e^2}\frac{1}{D_s N_s} = 1.6 \times 10^8 \frac{10^{-5}\frac{cm^2}{s}}{D_s}\frac{10^{14} cm^{-2}}{N_s} \quad (11)$$

Obviously, R_s can be very high, up to infinity at $N_s = 0$, but how low can it be? Can it be lower than the value corresponding to R_{min}?

Because of the basic nature of surface hydroxyls on alumina (point of zero charge, pzc ≈ 9.1),[41] in aqueous solution of neutral pH they are almost all charged (protonated). This gives an upper-limit estimate for the surface concentration of ions to be as high as that of hydroxyls, ~4×10^{14} cm^{-2}.[24,25] The majority of these hydroxyls are modified by linkers, and thus, the ion concentration is much smaller. According to Slevin and Unwin[42] the lateral proton diffusion coefficient along a stearic acid monolayer in LB films is similar to that of ion diffusion in water, $D_s \approx 10^{-5}$ cm^2/s. If we presume the same diffusion coefficient for our ions on the surface and their concentration on the order of 10^{14} cm^{-2}, the resulting $R_s \approx 1.6 \times 10^8$ Ω and $R \approx 5$ Ω would be much lower that the experimental limit R_{min}. Membrane resistance calculated for this diffusion coefficient of ions would remain less than R_{min} for surface ion densities N_s down to ~1.5% of the density of surface hydroxyls. Even though the surface density of ions is less than the density of unreacted hydroxyls, the latter can be above 10% for hydrophobic surfaces. Thus, there is a sufficient range of surface densities when the resistance of a 'dry' membrane can be lower than the experimental limit, R_{min}. In order to apply eq 11 to this case and others with higher resistances, a better estimate for N_s and D_s is needed for each case.

When the density of uncovered amine sites SiN in the mixed SiNH9/SiN monolayers of Figure 6 increases, the density of surface ions N_s increases as well. If the density of SiN is translated literally as N_s and D_s is taken to be constant at 10^{-5} cm^2/s, the calculated variation of membrane resistance, R:

$$R(\Omega) = x \times 5(\Omega) = \frac{\mathrm{SiN}}{\mathrm{SiN} + \mathrm{SiNH9}} \times 5(\Omega) \qquad (12)$$

as a function of the SiN fraction, x, is much more dramatic (dotted line in Figure 6) than the experimental one. The reason is that neither D_s nor the ratio between N_s and the density of SiN are constant. The correlation between N_s and the density of SiN is not linear because free volume and water are required within the monolayer for efficient stabilization of protonated amines (see Figure 7). For the same reason, diffusion of ions is extremely sensitive to the environment and would be highly partitioned toward hydrophilic groups such as residual surface amines in mixed SiNH9/SiN monolayers; ion transfer from one group to another would account for weak nonzero conductance. Most of the variations in Figure 6 occur in the range of small fraction of amines where the resistance for SiNH9/SiN membranes drops almost exponentially with increasing fraction of amines. In this regime, where amine sites are sparse and surrounded by hydrocarbons, the dependence of conductance on intersite distance dominates the overall behavior and resembles that of a salt in low-polarity solvents. In a hydrophobic monolayer that is made of a low dielectric constant hydrocarbon, dissociation of an ion pair, even when is formed, does not happen with 100% probability because of a strong Coulombic attraction, which drops off exponentially with distance, and at the Onsager radius[42] becomes equal to the thermal energy:

$$r_c = \frac{e^2}{4\pi\epsilon_0\epsilon k_B T} \qquad (13)$$

The Onsager radius, r_c, is inversely proportional to the dielectric constant, ϵ, and for $\epsilon = 2$ equals 29 nm. The dielectric constant near the monolayer bottom is likely higher than 2, but even for $\epsilon = 4$ the yield of dissociation for tightly bound ions is insignificant.[44] The ions are never 'free'; they are bound within the regions with fuzzy boundaries with dimension on the order of r_c. The conductivity increases when these regions overlap, which allow ions to jump from one counterion to another. The area encircled by the Onsager radius in a medium with $\epsilon = 4$ is about 50 nm^2, which is close to the experimental increment in the exponential fit for R from Figure 6.

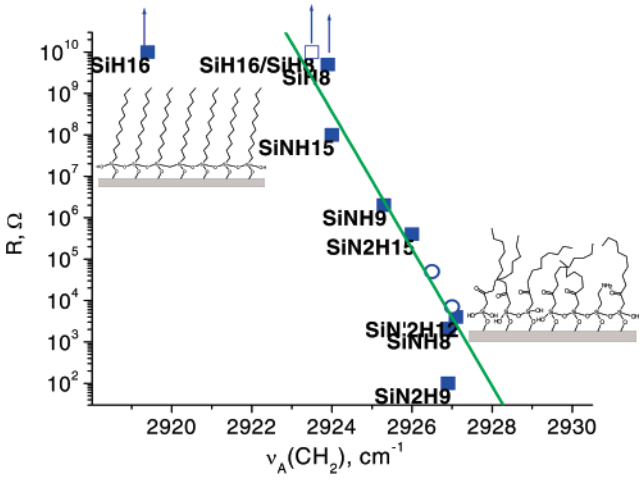

Figure 8. Correlation between the membrane resistance and the frequency of asymmetric CH_2 stretching, ν_A. Solid squares represent maximum coverage of the labeled monolayers and empty circles represent intermediate coverage of SiNH9 in SiNH9/SiN. The empty square is for a 50:50 mixture of SiH16/SiH8. The line is linear fit, $\ln R = 11\,170 - 3.81\nu_a(CH_2)$, to the points excluding SiH16 and SiH8.

In a more simplistic phenomenological approach one can contend that as long as the outermost part of the modifiers is hydrophobic, different linkers with the same ending group should interact similarly with water and the lack of its intrusion under the hydrophobic layer should translate into zero electrical conductance. Thus, the difference between modifiers arises primarily from variations in the packing quality of the monolayers. As Figure 4 demonstrates, the value of $\nu_a(CH_2)$ correlates well with the surface density of molecules and with the membrane resistance R for a series of long modifiers. We can try to extend this correlation to a broader class of aliphatic molecules with the anticipation that $\nu_a(CH_2)$ can provide a good measure of packing quality, which can decline because of either low surface density of molecules or their poor all-trans alignment. In other words, $\nu_a(CH_2)$ would 'scale' with the accessibility of the underlying oxide surface through imperfections of the hydrophobic layer. Indeed, as Figure 8 demonstrates, such a simplification has some merit similar to the previously reported correlation between transmittance through alkyl thiols on gold and their $\nu_a(CH_2)$ frequency.[36−39] The SiH16 modifier is unique in having very high impedance, for which we have only a lower limit value of 10^{10} Ω. If this point is ignored, the remaining ones can all be approximated by a single-exponential dependence: $\ln\{R/\Omega\} = 11170 - 3.81\nu_a(CH_2)$. The data point for the SiNH5 membrane was excluded, but it does not contradict the above dependence because of its high value of $\nu_a(CH_2) = 2933$ cm^{-1} and the correspondingly low $R < R_{min}$.

(41) Brown, G. E.; Henrich, V. E.; Casey, W. H.; Clark, D. L.; Eggleston, C.; Felmy, A.; Goodman, D. W.; Gratzel, M.; Maciel, G.; McCarthy, M. I.; Nealson, K. H.; Sverjensky, D. A.; Toney, M. F.; Zachara, J. M. *Chem. Rev.* **1999**, *99*, 77−174.

(42) Slevin, C. J.; Unwin, P. R. *J. Am. Chem. Soc.* **2000**, *122*, 2597−2602.

(43) Onsager, L. *Phys. Rev.* **1938**, *54*, 554.

(44) From Onsager's $\varphi_{diss} = \exp(-r_c/r_i)$ for ions initially separated by $r_i = 0.5$ nm $\varphi_{diss} < 10^{-12}$.

Fluorinated modifiers also provide a range of varying membrane resistances despite having almost identical contact angle with water. Even though their contact angle, $\theta_A \approx 150°$, is higher than that of the SiH16 modifier, the impedances for the corresponding membranes are less. It is not currently possible to evaluate whether or not the impedance variation can be correlated with the monolayer packing, because the IR absorbance for corresponding $\nu_a(CF_2)$ on alumina membranes falls out of the accessible range. Nevertheless, the results for these membranes emphasize the fact that a higher water contact angle of the membrane does not require a higher resistance.

We note that the phenomenon of surface conductance also explains the previously confusing behavior of mixed SiNH9/SiNspiropyran monolayers.[9] Despite the hydrophobic appearance of such monolayers with a *high* content of spiropyran, the resistance of the corresponding membranes was very low, on the order of 40 Ω, which was barely above the cell resistance of 15 Ω in that case (see Figures 4 and 5 in ref 9). The resistance drops to 15 Ω upon switching the spiropyran into the merocyanine form, as expected after intrusion of electrolyte. The reason for low membrane resistance in the region of high relative concentrations of spiropyran is similar to that depicted in Figure 6 of this paper. The bulky spiropyran molecules prevent some of the surface-bound amino groups from reacting with carboxyls during further functionalization, and they later serve as part of the conducting network. When the free amino group concentration is low enough, the resistance switching effect is maximal. This undesired effect could be rectified by a scheme where most of amines are neutralized.

Conclusions

We have demonstrated that nanoporous alumina membranes, the surfaces of which have been modified with hydrophobic monolayers of different types, despite being hydrophobic, do conduct electricity even when the pores are not filled with electrolyte. They do it via surface imperfections in the hydrophobic layer of the walls while still keeping the pores dry. The conductance increases with decreasing surface coverage and/or its quality, but is independent of electrolyte concentration and pH. It allows surface conductance of hydrophobic monolayer to be used for monitoring the extent of water intrusion into hydrophobic membranes.[27]

When a hydrophobic monolayer has a small portion of photoactive spiropyran that is insufficient to switch the surface to hydrophilic after spiropyran photoisomerization to merocyanine, the membrane resistance also becomes light dependent with a reversible increase of surface resistance. The evidence demonstrate that the likely mechanism of conductance is via hydrated surface hydroxyls and other water sensitive/ionizable groups such as primary and secondary amino groups of linkers. This interpretation is supported by the fact that resistance strongly correlates with the quality of coverage and pH dependence of water electrolyte intrusion into membrane. The latter can be related to the intensity and the frequency of the IR antisymmetric methylene stretching $\nu_a(CH_2)$ for groups in the tails of the surface modifiers. It appears that the ionizable groups are for the most part basic because intrusion of a strong base is not as significant as that of an acid. This interpretation is consistent with the nature of surface hydroxyls on alumina and amines of the linkers used.

Acknowledgment. This work was partially supported by a grant from the National Institutes of Health (NIH SCORE GM08136 to SS) and the National Science Foundation (CHE-0352599 to D.G.).

Supporting Information Available: IR spectra, details of contact angle, and impedance measurements. This material is available free of charge via the Internet at http://pubs.acs.org.

LA070038Q